Anthryl-Based Poly(phenylene ethynylene)s: Tuning Optical Properties with Diels−Alder Reactions

Eléna Ishow,† Jean Bouffard, Youngmi Kim, and Timothy M. Swager*

Department of Chemistry, Massachusetts Institute of Technology, 77 Massachusetts Avenue, Cambridge, Massachusetts 02139

Received August 17, 2006; Revised Manuscript Received September 10, 2006

ABSTRACT: Soluble anthryl-based conjugated poly(phenylene ethynylene)s (PPEs) have been synthesized using palladium-catalyzed Sonogashira−Hagihara cross-coupling polymerization reactions. Molecular weights up to 3.5×10^4 g·mol^{-1} were obtained, making them suitable for spectroscopic solution characterizations and thin film processing. The selective reactivity of these polymers as multidienes has been successfully demonstrated with strong dienophiles. Diels−Alder reactions proceed cleanly to completion with unhindered dienophiles such as *N*-alkylated maleimide derivatives. TGA analysis revealed thermal retro-Diels−Alder reactions at modest temperatures around 210 °C. Compared with their parent polymers, the cycloadduct polymers exhibited dramatic hypsochromic shifts of their emission and absorption maxima up to 80 nm along with a considerable quantum yield enhancement. These original anthryl-based polymers appear attractive as reactive conjugated materials whose optical properties can easily be tuned with quantitative Diels−Alder reactions.

Introduction

Poly(phenylene ethynylene)s (PPEs), based on fully π-conjugated shape persistent chain structures, are promising materials for a wide range of applications varying from electronic devices as electron or hole transport layers[1] to chemo-[2] and biosensors.[3] However, most of the polymers synthesized to date require UV excitation to affect luminescence, making them of limited use as in vivo biological sensors wherein the excitation can damage the living cells. Introduction of more delocalized and rigid structures such as anthracene can provide materials with red-shifted absorptions. However, these materials generally suffer from poor solubility due to strong $\pi-\pi$ inter- and intrachain interactions.[4] Appending dialkoxy or dialkyl chains onto aryl units embedded in the main chain dramatically improves PPE polymer solubility, but this well-known synthetic strategy is insufficient when high anthryl content is desired.[5,6] Following some of our past expertise in the synthesis of soluble high-molecular-weight conjugated polymers, we have turned our efforts toward the synthesis of anthryl monomers fused to triptycenyl substituents.[2b−c,7] These designs allow for the incorporation of three-dimensional structures that prevent strong interchain interactions and thereby promote high solubility without disruption of the desired electronic effects of the anthryl units. We herein report the successful synthesis of highly soluble anthryl-based PPEs whose high anthryl content provides green- to red-emitting materials. Full π-conjugation of anthryl units within the main polymer chain further allows for the tuning of polymer optical properties via Diels−Alder reactions to an unusual extent. This is in contrast with most polymers containing anthryl units that are connected by saturated linkages and do not display large changes in their electronic properties upon cycloadduct formation.[8] To test the Diels−Alder reactivity of these novel polymers in solution, we have investigated various *N*-substituted maleimides dienophiles[3a,9] that are also often used for surface biofunctionalization.[10] Comparative studies of the polymers using ^{1}H NMR, absorption, and emission spectroscopies before and after Diels−Alder reactions underscore the potential of these polymers to act as tunable emissive materials.

* Corresponding author. E-mail: tswager@mit.edu.

† Current address: ENS Cachan, PPSM-UMR CNRS 8531, 61 Avenue du Président Wilson, 94235 Cachan Cedex, France. E-mail: ishow@ppsm.ens-cachan.fr. Telephone: +33 1 47 40 76 60. Fax: +33 1 47 40 24 54.

Results and Discussion

Synthesis and Structural Characterizations of Anthryl-Based Polymers. The formation of the investigated anthryl-based polymers necessitated the synthesis of new diethynyl monomers as depicted in Scheme 1. Monomers **3** and **5** were obtained in four key synthetic steps. First, anthracene and the commercially available 1,4-anthraquinone were reacted in a Lewis-acid-catalyzed Diels−Alder cycloaddition.[11] Acid-catalyzed rearomatization of the diketo cycloadduct produced the hydroquinone, which could be oxidized in situ by potassium bromate to afford **1**.[12] Alternatively, anthracene derivative **4** could be produced when the Diels−Alder adduct was sequentially reacted with $LiAlH_4$ and TsCl/pyridine.[13] The diethynyl monomer **3** was obtained by the addition of lithium trimethylsilylacetylide to the quinone, followed by tin chloride reduction and alkaline desilylation in the presence of KOH in THF/MeOH. Monomer **5** was produced by bromination of the anthracene derivative **4** with NBS in the dark. The diethynyl monomer **8** was obtained from a cycloaddition reaction between dimethylacetylenedicarboxylate (DMAD) and 6,13-bis(triisopropylsilylethynyl)pentacene (**6**),[14] followed by desilylation (Scheme 2). Monomers **3**, **5**, and **8** were used in a Sonogashira−Hagihara cross-coupling polymerization with one equivalent of their respective hexadecyloxyaryl monomers in the presence of catalytic CuI and $Pd(PPh_3)_4$ in a deoxygenated solution of diisopropylamine and toluene (1:3 v/v). The best results were obtained with extended (3 days) reaction times at 65 °C. Formation of the conjugated polymer can be detected visually even in the early stages of the reaction by a bright-orange fluorescence observed under UV irradiation. The corresponding polymers **1,4-TPPE**, **9,10-TPPE**, and **1,4-EPPE** were precipitated by slow addition of the reaction mixture into a large volume of well-stirred methanol. The precipitates were washed and subsequently purified by Soxhlet extraction with acetone.

10.1021/ma061901g CCC: $33.50
Published on Web 10/20/2006

Scheme 1. Synthetic Pathway to Polymers 1,4-TPPE and 9,10-TPPE

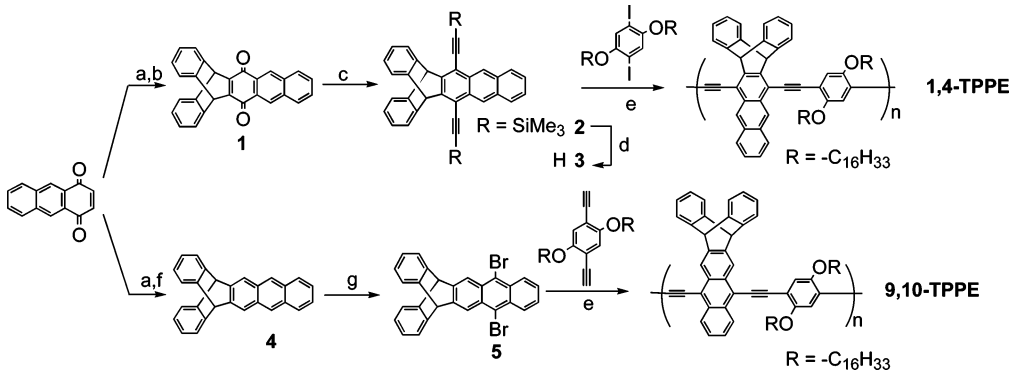

(a) i-Anthracene, $AlCl_3$, CH_2Cl_2, RT, 1 h; ii-HCl. (b) $KBrO_3$, AcOH rflx. (c) i-^{n}BuLi, trimethylsilylacetylene, THF, 0 °C; ii-$SnCl_2$, AcOH. (d) KOH, THF−MeOH, RT. (e) $Pd(PPh_3)_4$, CuI, 1:3 ^{i}Pr$_2$NH/toluene, 65 °C, 3 d. (f) i-$LiAlH_4$, THF, Et_2O, 0 °C, 1 h; ii-TsCl, pyridine, RT, 3 d. (g) NBS, DMF, RT, 1 h.

Scheme 2. Synthetic Pathway to Polymer 1,4-EPPE

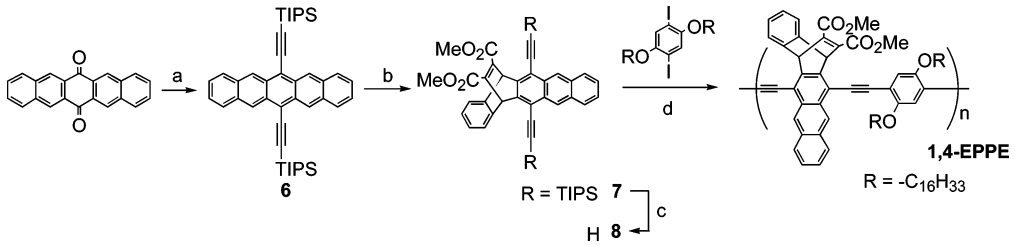

(a) i-^{n}BuLi, triisopropylsilylacetylene, THF, 0 °C; ii-$SnCl_2$, AcOH, RT, 24 h. (b) 1 equiv dimethylacetylenedicarboxylate, toluene, 100 °C, 15 min. (c) ^{n}Bu$_4$NF, THF, RT. (d) $Pd(PPh_3)_4$, CuI, 1:3 ^{i}Pr$_2$NH/toluene, 65 °C, 3 d.

Table 1. Structural and Thermal Characteristics of Anthryl-Based Parent and Cycloadduct Polymers

polymer	M_n (g·mol^{-1})[a]	M_w (g·mol^{-1})[a]	DP$_n$[a]	PDI[a]	T_g (°C)[b]
1,4-TPPE	37 000	86 800	45	2.3	207
1,4-EPPE	36 000	97 300	35	2.7	181
9,10-TPPE	10 100	37 500	9.6	3.5	124
9,10-PPE[6a]	n.a.	n.a.	10.8[c]	n.a.	n.a.
1,4-addMe	38 000	82 000	35	2.1	57

[a] Determined by GPC in THF with PS as narrow standards. [b] DSC analyses with a 10 °C·min^{-1} temperature gradient. [c] For elemental analyses, see ref 6a.

As mentioned earlier, previous conjugated anthryl-based polymers that lack triptycenyl substituents have limited solubility.[5] All of the anthryl polymers described here are readily soluble in most common chlorinated solvents, with THF and toluene being qualitatively judged to be the best solvents. This feature is attributed to the triptycenyl groups, which by virtue of their three-dimensional shape persistent structure prevent strong intermolecular $\pi-\pi$ aggregations.[6a] GPC analyses were performed in THF and revealed similar results for polymers **1,4-TPPE** ($M_n = 3.7 \times 10^4$ g·mol^{-1}, DP = 45, and PDI = 2.3) and **1,4-EPPE** ($M_n = 3.6 \times 10^4$ g·mol^{-1}, DP = 35, and PDI = 2.1), which suggests comparable reactivity/purity of both monomers (Table 1). Polymer **9,10-TPPE** was only obtained as a low-molecular-weight M_n of 1.0×10^4 g·mol^{-1} material (DP ≈ 9.6). The glass transition temperatures T_g of **1,4-TPPE** and **1,4-EPPE** were found by differential scanning calorimetry (DSC) to be 207 °C and 181 °C, respectively. These T_g values differ from that for **9,10-TPPE** measured at 124 °C, perhaps reflecting reduced inter- and intrachain interactions for **9,10-TPPE** relative to polymers containing 1,4-grafted anthryl units.

Comparative Spectroscopic Studies of 1,4-EPPE, 1,4-TPPE and 9,10-TPPE. The solution absorption spectra of **1,4-EPPE, 1,4-TPPE**, and **9,10-TPPE** exhibited maxima at $\lambda_{max} = 502$, 501, and 521 nm, respectively, assignable to $\pi-\pi^*$ transitions (Figure 1, Table 2). There is noticeable red-shifting for **9,10-TPPE** owing to the larger electronic delocalization with the anthryl units. In contrast to **9,10-TPPE**, the 1,4-anthryl branched polymers exhibited an additional electronic transition with vibrational structure at 381 and 361 nm for **1,4-TPPE** and 381 nm for **1,4-EPPE**, which is characteristic of $\pi-\pi^*$ anthryl-based electronic transitions.

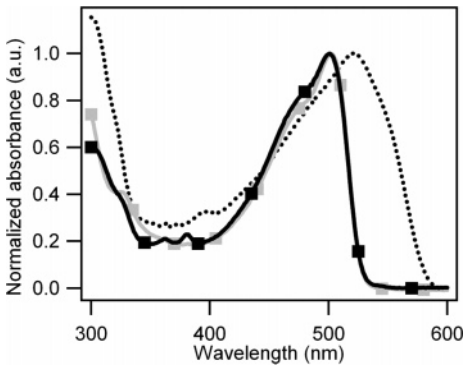

Figure 1. Normalized absorption spectra in $CHCl_3$ solution of **1,4-TPPE** (black, with squares), **1,4-EPPE** (gray, with squares), and **9,10-TPPE** (dotted).

The similarity between the **1,4-TPPE** and **1,4-EPPE** spectra reveals a weak influence of the peripheral substituents in the [2.2.2] bicyclic ring system (phenyl for **1,4-TPPE** and diester-alkene for **1,4-EPPE**) on the polymer's band gap. These results are in accord with recent studies on PPVs wherein similar substitutions were found to affect the polymer reduction potential but not its electronic spectra.[15] The emission spectra of polymers **1,4-TPPE**, **1,4-EPPE**, and **9,10-TPPE** in chloroform solution display a single band with vibrational structure typical of PPEs (Figure 2). As expected, on the basis of previous PPV studies,[14] the emission spectra of **1,4-TPPE** and **1,4-EPPE** both appear very similar, with a Stokes shift of 40 nm, maxima at 519 and

Table 2. UV−Vis Absorption and Emission Properties of Anthryl-Based Parent and Cycloadduct Polymers

	abs λ_{max} (nm)		em λ_{max} (nm)			
polymer	in $CHCl_3$	thin film[a]	in $CHCl_3$	thin film[a]	τ (ns)[b]	Φ_f[b]
1,4-TPPE	501, 381, 361	533, 384, 363	558, 519	589, 543	0.71	0.35[c]
1,4-EPPE	502, 381, 326	534, 334	559, 520	590, 544	0.76	0.33[c]
9,10-TPPE	521, 395	533	618, 570	638, 593	1.16	0.45[d]
9,10-PPE[6a]	543	n.a.	590	n.a.	1.00	0.05[6a]
1,4-addMe	426, 337	448, 340	541, 494, 457	535, 498, 463	0.48	0.70[e]

[a] 50 nm thick films. [b] In $CHCl_3$ solution. Quantum yield measured toward: acridine yellow in EtOH ($\Phi_f = 0.47$). [c] Rhodamine 6G in EtOH ($\Phi_f = 0.95$). [d] Quinine sulfate in 0.1 mol·L^{-1} H_2SO_4 ($\Phi_f = 0.53$).[e]

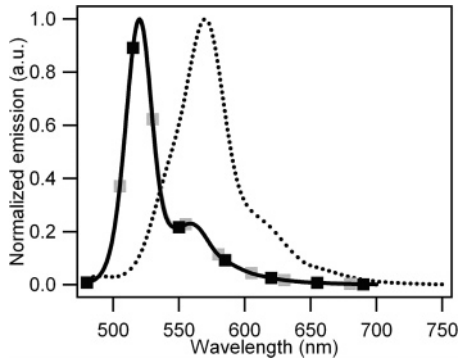

Figure 2. Normalized emission spectra in $CHCl_3$ solution **1,4-TPPE** (black, with squares), **1,4-EPPE** (gray, with squares), and **9,10-TPPE** (dotted).

520 nm, and vibrational bands at 558 and 559 nm, respectively. The emission maximum of **9,10-TPPE** is at 570 nm and has a similar Stokes shift of 50 nm (Table 2).

The similarities of **1,4-TPPE**, **1,4-EPPE** extend to their respective emission quantum yields Φ_f of 0.35 and 0.33 and fluorescence lifetimes τ_f of 0.71 ns and 0.76 ns, respectively. In contrast, the emission characteristics of **9,10-TPPE** are significantly different with higher $\Phi_f = 0.45$ and $\tau_f = 1.16$ ns. These materials differ from **9,10-PPE**,[6a] which is devoid of [2.2.2] bicyclic structures (Scheme 3) and displays a τ_f of 1 ns but a dramatically lower quantum yield of 0.05 caused by strong $\pi-\pi$ stacking interactions. Hence the bulky triptycenyl groups are successful at separating the π-conjugated main chains with high quantum yields. In thin films, polymers **1,4-TPPE**, **1,4-EPPE**, and **9,10-TPPE** underwent a systematic 30 nm bathochromic shift in absorption and emission, which is likely the result of a more extended planar conformation that is promoted by the dense packing of the polymers and weak interpolymer electronic interactions.

Diels−Alder Reactivity of Anthryl-Based TPPE Polymers. *Cycloadduct Synthesis.* Given the high structural and electronic similarities between **1,4-TPPE** and **1,4-EPPE**, we focused our studies on Diels−Alder adduct formation with *N*-substituted maleimide dienophiles reacting with **1,4-TPPE** and compared its reactivity with **9,10-TPPE**. Reactions were performed with a 100-fold excess of *N*-methylmaleimide and/or *N*-phenylmaleimide in dry and air-free xylene solution at 120−130 °C for 3 h to prevent moisture from affecting the endo/exo stereoselectivity and minimize the risks of oxidative degradation.[16] Reactions on **1,4-TPPE** yielded cycloadduct polymers **1,4-addMe** and **1,4-addPh**, whereas no Diels−Alder reaction was detected for **9,10-TPPE** (Scheme 4). It is worth noting that solubility of the final polymer cycloadducts is considerably improved relative to that of the parent polymer **1,4-TPPE**. This reveals the effectiveness of rigid cyclic scaffolds at reducing the polymer aggregation due to $\pi-\pi$ interactions that are inherent to most conjugated polymers.

^{1}H NMR Characterizations. ^{1}H NMR spectroscopy was used to quantify the progress of the Diels−Alder reaction with **1,4-TPPE**. Cycloadduct formation is accompanied by new peaks appearing at high field (NCH_3, H_g) coming from maleimide along with an upfield shift of H_e and H_d proton resonances (Figure 3). Shielding of H_d resonance is especially dramatic, with the peak shifting from $\delta = 9.08$ ppm to $\delta = 5.43$ ppm with Diels−Alder cyclization, owing to the loss of aromatic character of the vicinal carbon atoms (Figure 3).

On the basis of the integration of the H_d original peak on cycloadduct ^{1}H NMR spectra, we estimated a 40% conversion of **1,4-TPPE** into its cycloadduct when reacting with *N*-phenylmaleimide (**1,4-addPh)** and 100% conversion with *N*-maleimide (**1,4-addMe**). In the latter, we observed the complete disappearance of the original H_d signals and a 1:1 integration ratio of cycloadduct aliphatic H_g protons coming from *N*-methylmaleimide and protons H_d and H_c linked to the reacted anthryl units. Clearly the Diels−Alder reaction with **1,4-TPPE** is more efficient with unhindered maleimide dienophiles.

The ^{1}H NMR spectrum displays two sets of peaks instead of one for both H_c and H_d at $\delta = 6.24$, 5.43 ppm and $\delta = 6.15$, 5.53 ppm. The integrations of these two sets of protons were 64% and 36%, respectively, relative to the other aromatic protons. The cycloaddition is expected to yield two stereoisomers, hence these two sets represent the exo- and endo-isomeric units in the cycloadduct polymer **1,4-addMe**. To determine the identity of the prevalent isomeric unit, we synthesized two model compounds by reacting *N*-maleimide with the triisopropyl analogue of monomer **2** (TIPS groups were used instead of TMS to better mimic steric repulsions caused by the PPE chain in the polymer) using the same reaction conditions as those for **1,4-addMe**. Two stereoisomerically pure compounds **cyclo1** and **cyclo2** were obtained, and their ^{1}H NMR spectra were analyzed (Figure 4). Given the complexity in the aromatic region of the **1,4-addMe**, we focused our attention on four sets of aliphatic protons only, namely H_c, H_d, H_g, and NCH_3 and the analogous

Scheme 3. Structure of the Anthryl-Based Polymers

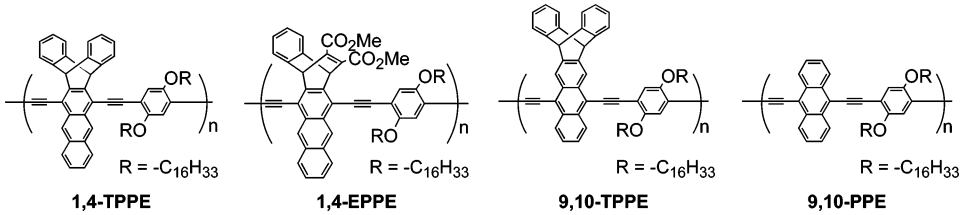

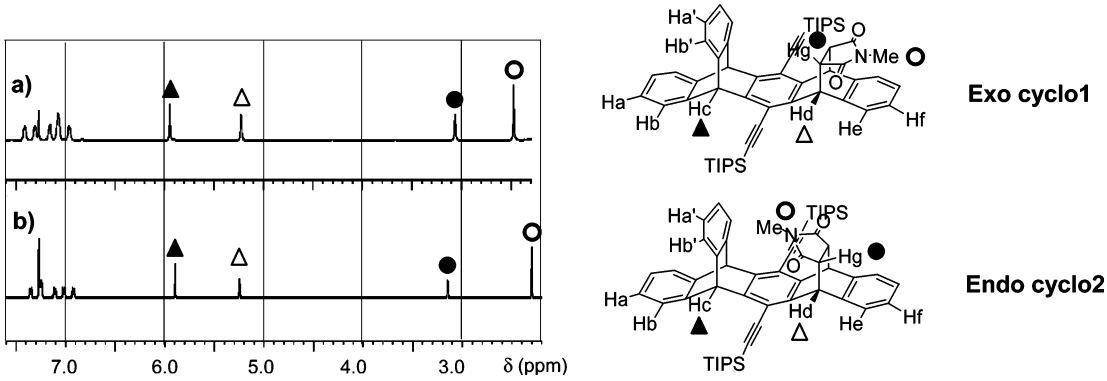

Figure 3. ^{1}H NMR (400 MHz) spectra in $CDCl_3$ of (a) **1,4-TPPE** and (b) **1,4-addMe**.

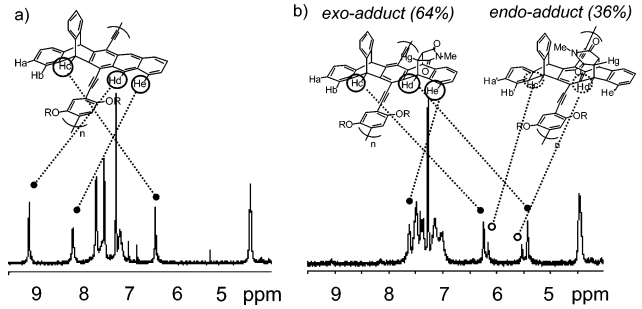

Figure 4. ^{1}H NMR spectra (400 MHz, $CDCl_3$) of (a) **exo cyclo1** and (b) **endo cyclo2**.

signals for models **cyclo1** and **cyclo2**, the corresponding protons that resonated at 5.94, 5.22, 3.06, and 2.47 ppm and 5.90, 5.25, 3.15, and 2.30 ppm, respectively. The NCH_3 protons of the exo isomer lie above one phenyl ring only, whereas NCH_3 protons of the endo isomer are located above both the tolane ring and one of the two triptycenyl phenyl rings. Conversely, H_g for the exo isomer is located above the tolane ring. Because protons placed above an aromatic ring experience magnetic shielding, the NCH_3 signal for the exo isomer is expected to appear at lower field than that for the endo isomer and **cyclo1** ($\delta(NCH_3) = 2.47$ ppm, $\delta(Hg) = 3.06$ ppm) and **cyclo2** ($\delta(NCH_3) = 2.30$ ppm, $\delta(Hg) = 3.15$ ppm) corresponded to the exo and endo isomers, respectively. Considering the signals of the exo-**cyclo1**, H_c and H_d protons have higher and lower respective chemical shifts than the H_c and H_d signals of the endo-**cyclo2**. Hence we assign the **1,4-TPPE** exo/endo units' ratio as 64%:36% by considering the H_c (H_c') and H_d (H_d') protons. This stereoselective feature agrees with what we might have suspected initially on steric grounds.

*Structural and Thermal Characterizations of **1,4-addMe**.* Cycloadduct polymer **1,4-addMe** has increased solubility relative to the parent polymer **1,4-TPPE**. GPC analyses performed in THF afforded $M_n = 3.8 \times 10^4$ g·mol^{-1}, $DP_n = 33$, and PDI = 2.1. The slight apparent decrease in M_n and DP_n relative to **1,4-TPPE** may be attributed to differences in chain stiffness (hydrodynamic radius) (Table 1). DSC measurements reveal a dramatic drop of the glass transition temperature from 207 °C for the parent polymer to 57 °C for **1,4-addMe**, which reflects a removal of the strong anthryl $\pi-\pi$ intermolecular interactions in **1,4-TPPE**.

Thermogravimetric analyses (TGA) allowed for the determination of the temperature onset for thermal induction of retro-Diels−Alder reactions (Scheme 4). Upon heating a sample of **1,4-addMe** at a 10 °C·min^{-1} rate from 25 to 700 °C under nitrogen, weight loss of 7% was observed starting at 247 °C, which is reasonably in good agreement with the theoretical 10%

Scheme 4. Diels−Alder Reaction of 1,4-TPPE and 9,10-TPPE with Various *N*-substituted Maleimides

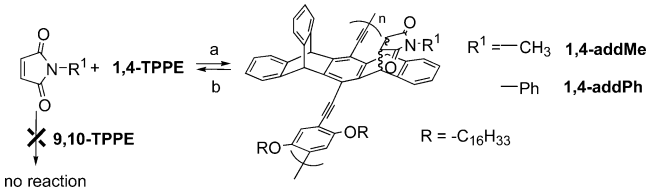

(a) Xylene, 130°C, 3 h. (b) Heating at $T > 200$ °C under N_2.

loss for complete cycloreversion of all of the *N*-methylmaleimide moieties (Figure 5). Control experiments on the parent polymer **1,4-TPPE** indicated no significant weight loss below 380 °C. The retro-Diels−Alder **1,4-addMe** is comparable to that of the cycloadduct monomer issued from cycloaddition between anthracene and *N*-methylmaleimide, which is thermally induced at 267 °C.

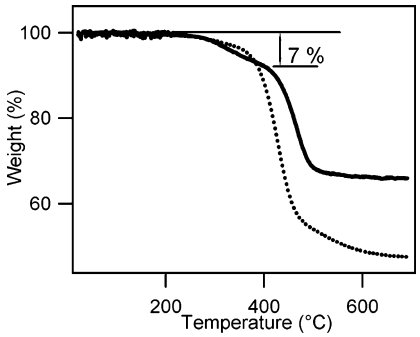

Figure 5. TGA analyses of **1,4-TPPE** (dotted line) and **1,4-addMe** (solid line) under N_2 (10 °C·min^{-1} heating rate).

Comparative Spectroscopic Studies of 1,4-addMe and 1,4-TPPE. Absorption and emission spectra of cycloadduct polymer **1,4-addMe** dramatically differ from those of the parent polymer **1,4-TPPE** (Figure 6). The maximum absorption and emission wavelengths of **1,4-addMe** are 426 and 494 nm, respectively, both being blue-shifted by 70−80 nm (Table 2) relative to **1,4-TPPE**. These large changes can easily be explained through the removal of the electronic delocalization provided by the anthryl units. This can be understood based upon the fact that the aromatic stabilization is lower in a ring in an anthryl system relative to an isolated phenyl group. Strongly aromatic phenylene polymers restrict the delocalization of electrons and will have an increased HOMO−LUMO gap relative to anthryl homologues.[17] The emission quantum yields in solution rise from $\Phi_f = 0.31$ to 0.70 when the parent polymer **1,4-TPPE** is transformed to **1,4-addMe** (Table 2). There are two reasons for this increase. On the basis of the energy gap law, we naturally

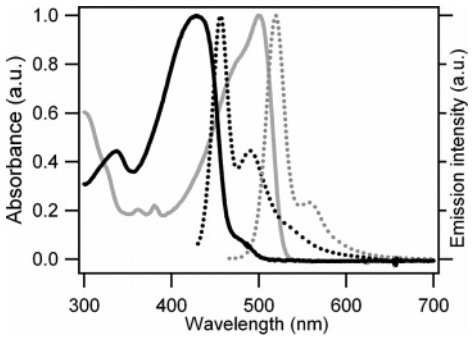

Figure 6. Absorption (solid lines) and emission (dotted lines) spectra in $CHCl_3$ solution of **1,4-TPPE** (gray), **1,4-addMe** (black, $\lambda_{exc} = 425$ nm).

expect a weaker coupling between the vibrational wave functions of the ground and excited electronic states with a larger band gap, hence Diels−Alder Adduct formation lowers the nonradiative rate. In addition, the [2.2.2] scaffold prevents strong interchain π-interactions that are responsible for self-quenching.

This latter effect is enhanced in spin-cast thin films wherein the absorption spectrum of **1,4-addMe** has a shape similar to that of the solution spectrum and the corresponding maximum is about 20 nm red-shifted. The emission spectra for **1,4-addMe** is broadened and exhibits a lower bathochromic shift and different relative vibronic transition intensities. The ratio of both the emission maxima at 494 and 457 nm was equal to 0.5 in solution, but in thin films, this ratio increased to 2. These differences may be the result of an emitting excimer or energy transfer.[18] A better understanding of this effect is the subject of ongoing research in our group.

Conclusion

In conclusion, anthryl-based poly(arylene ethynylene)s were successfully obtained with DPs varying from 12 to 45 using a palladium-catalyzed cross-coupling reaction. Their high solubility in common organic solvents was related to the presence of triptycenyl groups as peripheral solubilizing groups, which permitted solution spectroscopic investigations of high-anthryl-content conjugated polymers. Upon Diels−Alder reaction with *N*-methylmaleimide, quantitative conversion of the parent polymer **1,4-TPPE** into its cycloadduct **1,4-addMe** was obtained. ^{1}H NMR experiments evidenced the formation of a stereorandom polymer, with the less crowded exo unit prevailing at 64%. This cycloaddition induces dramatic blue-shifts in absorption and emission (up to 80 nm). Finally, the planar anthryl units are prone to aggregation and emission self-quenching, but the polymer resulting from the cycloaddition provides a 125% increase in the emission quantum yield. These anthryl-based PPE polymers constitute a new family of materials whose emission can be chemically modified in intensity (quantum yield enhancement) but also in energy (hypsochromic shift). We envisage the possibility of creating in solid films an in situ optical gradient by reaction with dienophiles.

Acknowledgment. This research has been financially supported by the National Science Foundation, French Ministry of Research and Education, CNRS, and NSERC (J. B.). Staff of the MIT Department of Chemistry Instrumentation Facility is gratefully thanked for providing analytical instrumentations and training of high quality.

Supporting Information Available: Full experimental details for the synthesis of monomers and polymers, and description of the utilized equipment. This material is available free of charge via the Internet at http://pubs.acs.org.

References and Notes

(1) (a) Meier, H.; Mühling, B.; Kolshorn, H. *Eur. J. Org. Chem.* **2004**, *5*, 1033−1042. (b) Egbe, D. A.; Carbonnier, B.; Ding, L. M.; Mühlbacher, D.; Birckner, E.; Pakula, T.; Karasz, K. E.; Grummt, U. W. *Macromolecules* **2004**, *37*, 7451−7463. (c) Kokil, A.; Shiyanovskaya, I.; Singer, K. D.; Weder, C. *Synth. Met.* **2003**, *138*, 513−517.

(2) (a) DiCesare, N.; Pinto, M. R.; Schanze, K. S.; Lakowicz, J. R. *Langmuir* **2002**, *18*, 7785−7787. (b) Yang, J.-S.; Swager, T. M. *J. Am. Chem. Soc.* **1998**, *120*, 11864−11873. (c) Williams, V. E.; Swager, T. M. *Macromolecules* **2000**, *33*, 4069−4073. (c) McQuade, D. T.; Pullen, A. E.; Swager, T. M. *Chem. Rev.* **2000**, *100*, 537−574.

(3) (a) Rabjohns M. A.; Hodge, P.; Lovell, P. A. *Polymer* **1997**, *38*, 3395−3407. (b) Li, T.; Chem, J.; Misuishi, M.; Miyashita, T. *J. Mater. Chem.* **2003**, *13*, 1565−1569.

(4) (a) Disney, M. D.; Zheng, J.; Swager, T. M.; Seeberger, P. H. *J. Am. Chem. Soc.* **2004,** *126*, 13343−13346. (b) Wilson, J. N.; Wang, Y. Q.; Lavigne, J. J.; Bunz, H. F. *Chem. Commun.* **2003**, 1626−1627.

(5) (a) Bunz, U. H. *Chem. Rev.* **2000**, *100*, 1605−1644. (b) Weder, C.; Wrighton, M. S. *Macromolecules* **1996**, *29*, 5157−5165. (c) Egbe, D. A.; Bader, C.; Nowotny, J.; Günther, W.; Klemm, E. *Macromolecules* **2003**, *36*, 5459−5469.

(6) (a) Swager, T. M.; Gil, C. J.; Wrighton, M. S. *J. Phys. Chem.* **1995**, *99*, 4886−4893. (b) Sinigersky, V.; Müllen, K.; Klapper, M.; Schopov, I. *Adv. Mater.* **2002**, *12*, 1058−1060.

(7) (a) Amara, J. P.; Swager, T. M. *Macromolecules* **2004**, *37*, 3068−3069. (b) Long, T. M.; Swager, T. M. *Adv. Mater.* **2001**, *13*, 601−604

(8) (a) Lei, X.; Porco, J. A. *Org. Lett.* **2004**, *6*, 795−798. (b) Ilhan, F.; Tyson, D. S.; Meador, M. A. *Chem. Mater.* **2004**, *16*, 2978−2980. (c) Shenhar, R.; Sanyal, A.; Uzun, O.; Rotello, V. M. *Macromolecules* **2004**, *37*, 92−98.

(9) (a) Gheneim, R.; Perez-Berumen, C.; Gandini, A. *Macromolecules* **2002**, *35*, 7246−7253. (b) Atherton, J. C.; Jones, S. *Tetrahedron Lett.* **2002**, *43*, 9097−9100. (c) Tobia, D.; Harrison, R.; Phillips, B.; White, T. L.; DiMare, M.; Rickborn, B. *J. Org. Chem.* **1993**, *58*, 6701−6706. (d) Vargas, M.; Kriegel, R. M.; Collard, D. M.; Schiraldi, D. A. *J. Polym. Sci., Part A: Polym. Chem.* **2002**, *40*, 3256−3263.

(10) (a) Park, S.; Lee, M. R.; Pyo, S. J.; Shin, I. *J. Am. Chem. Soc.* **2004**, *126*, 4812−4819. (b) Xiao, S. J.; Brunner, S.; Wieland, M. *J. Phys. Chem. B* **2004**, *108*, 16508−16517.

(11) Bartlett, P. D.; Ryan, M. J.; Cohen, S. G. *J. Am. Chem. Soc.* **1942**, *64*, 2649−2653.

(12) (a) Yang, J.-S.; Liu, C.-P.; Lin, B.-C.; Tu, C.-W.; Lee, G.-H. *J. Org. Chem.* **2002**, *67*, 7343−7354. (b) Wasielewski, M. R.; Niemczyk, M. P.; Johnson, D. G.; Svec, W. A.; Minsek, D. W. *Tetrahedron* **1989**, *45*, 4785−4806. (c) Wiehe, A.; Senge, M. O.; Kurreck, H. *Liebigs Ann./Recl.* **1997**, 1951−1963.

(13) Patney, H. K. *Synthesis* **1991**, 694−696.

(14) (a) Anthony, J. E.; Eaton, D. L.; Parkin, S. R. *Org. Lett.* **2002**, *4*, 15−18. (b) Kim, Y.; Whitten, J. E.; Swager, T. M. *J. Am. Chem. Soc.* **2005**, *127*, 12122−12130.

(15) Kim, Y.; Zhu, Z.; Swager, T. M. *J. Am. Chem. Soc.* **2004**, *126*, 452−453.

(16) Cativiela, C.; Garcia, J. I.; Mayoral, J. A.; Salvatella, L. *Chem. Soc. Rev.* **1996**, 209−218.

(17) (a) Schenning, A. P.; Tsipis, A. C.; Meskers, S. C.; Beljonne, D.; Meijer, E. W.; Brédas, J. L. *Chem. Mater.* **2002**, *14*, 1362−1368. (b) Hoppe, H.; Egbe, D. A.; Mühlbacher, D.; Sariciftci, N. S. *J. Mater. Chem.* **2004**, *14*, 3462−3467.

(18) Kim, Y.; Bouffard, J.; Kooi, S. E.; Swager, T. M. *J. Am. Chem. Soc.* **2005**, *127*, 13726−13731.

MA061901G